Synthesis of L2Ni(ORF)2 (RF=C(CF3)3) Complexes and their Reactivity in Ethylene Oligomerization

Julien Petit, Nathalie Saffon-Merceron, Lionel Magna, Nicolas Mézailles

Synthetic of $L_2Ni(OR^F)_2$ (R^F=$C(CF_3)_3$) complexes and their reactivity in ethylene oligomerization.

Julien Petit,[a,b] Nathalie Saffon-Merceron,[c] Lionel Magna,*[b] Nicolas Mézailles.*[a]

[a] Laboratoire Hétérochimie Fondamentale et Appliquée, UMR 5069 CNRS, Université Paul Sabatier, 118 Route de Narbonne ; 31062 Toulouse, France.

[b] IFP Energies Nouvelles Rond-point de l'échangeur de Solaize, BP3, 69360 Solaize, France.

[c] Institut de Chimie de Toulouse ICT – FR2599, Université Paul Sabatier, 118 Route de Narbonne, 31062 Toulouse, France.

ABSTRACT: A family of $L_2Ni(OR^F)_2$ (L_2 : $(Cy_3PO)_2$ **6**, dcpmS **7**, dppf **11**, $bipyMe_2$ **12** ; R^F=$C(CF_3)_3$) complexes is synthesized via selective substitution of two equivalents of $(DME)NaOR^F$ from the homoleptic $[Ni(OR^F)_4][Na(DME)]_2$ complex **1**, all characterized by ^{19}F, ^1H NMR and SCXRD analyses as well as elemental analyses. These $L_2Ni(OR^F)_2$ precursors, activated by two equivalents of $PhF{\rightarrow}Al(OR^F)_3$, were active in ethylene oligomerization with selectivity towards butenes up to 97% and activities ranging from 10 to 50 $kg_{C2H4}.g_{Ni}.h^{-1}$. Mechanistic investigations, involving experiments with C_2H_4/C_2D_4 (1/1) coupled with GC-MS analysis, revealed the formation of a Ni-H fragment in the catalytic process. The $L_2Ni(OR^F)_2$/2PhF→$Al(OR^F)_3$ catalytic system thus dimerizes ethylene through a Cossee-Arlman mechanism.

INTRODUCTION

Linear alpha olefins (LAOs) represent an important market, with an annual production estimated at 6.2 million tons in 2018.[1] Depending on their alkyl chain length, LAOs can be used as starting materials in various applications such as comonomers in the polymer industry, detergents, surfactants or lubricants.

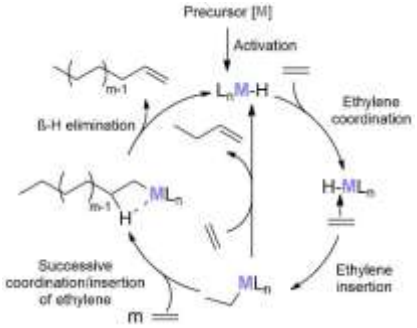

Scheme 1 – Cossee-Arlman mechanism.

Catalytic ethylene oligomerization represents a major access to such molecules containing an even number of carbon atoms. Homogeneous catalysis has been very successful, although obtaining a high selectivity in the oligomers remains challenging. Two mechanisms, the "Cossee-Arlmann" mechanism (Scheme 1)[2] and the "metallacyclic" mechanism (Scheme 2),[3] promote the oligomerization process. The first pathway is known to involve a metal-hydride/alkyl bond while the second needs a metallic fragment able to promote oxidative coupling of two ethylene molecules. Amongst the different metal used,[4–6] nickel based-catalysts certainly took part in one of the success stories in this domain, i.e. the SHOP process.[7,8] Since then, many other Ni-catalysts have been developed.[9]

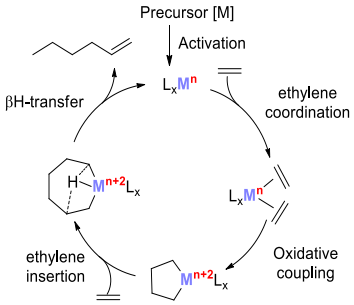

Scheme 2 – Metallacyclic mechanism.

Up-to-now, the limited selectivity observed with nickel-based catalysts is mainly rationalized through a Cossee-Arlman mechanism with the active species featuring a Ni-H or Ni-C bond.[9,10] Nonetheless, only few nickel catalysts have been reported to be highly selective in ethylene dimerization to butenes/1-butene.[11–17] In these cases, the precise mechanism has not been studied. Yet, in general, catalysts that follow a metallacyclic mechanism are known to be much more selective towards a unique 1-alkene,[18–25] Moreover, it has been shown that nickel was able, with activated alkenes such as tetrafluoroethylene (TFE), norbornadiene or dimethylcyclopropene, to achieve an oxidative coupling to reach metallacyclic complexes (Scheme 3, top).[26–28] In addition, Grubbs showed that butenes can be obtained from a mixture of $(Cy_3P)_2NiCl_2$ and 1,4-dilithiobutane, through the proposed decomposition of the nickellacyclopentane.[29] Binger reported few years after that an isolated nickellacycle yielded 1-butene upon heating at 165°C (Scheme 3, down).[30]

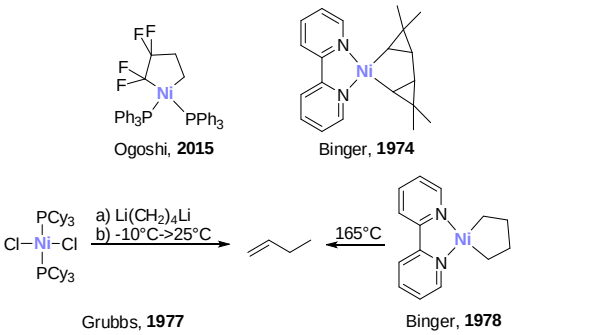

Scheme 3 – Top: isolated nickellacycles after oxidative coupling. Down: formation of 1-butene from the decomposition of nickellacyclopentane.

In 2015, Ogoshi and co-workers reported the first example of co-oligomerization of ethylene and TFE with a nickel complex going through a metallacycle.[31] They showed that a metallacyclic intermediate was not accessible from $(Ph_3P)_2Ni(C_2H_4)$ and ethylene. But when adding TFE on $(Ph_3P)_2Ni(C_2H_4)$, the oxidative coupling was accessible (Scheme 3) due to electronic properties of TFE. When the nickellacycle $(Ph_3P)_2Ni(CF_2CF_2CH_2CH_2)$ was placed under an ethylene atmosphere in C_6D_6 the production of tetrafluoro-1-hexene was observed (Scheme 4) and proved to result from a metallacylic pathway.

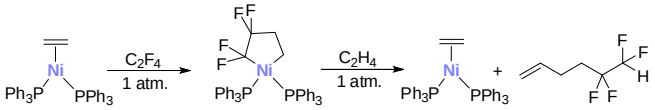

Scheme 4 – Synthesis 5,5,6,6-tetrafluoro-1-hexene through a metallacyclic isolated intermediate.

In 2013, Le Floch, Adamo and co-workers reported a theoretical study focusing on their highly selective nickel catalyst (butenes, 97%).[12,32] They considered the two possible mechanisms for ethylene oligomerization and showed that both were compatible with the observed selectivity. Importantly, they highlighted that oxidative coupling was not kinetically accessible starting from $[(P,N)Ni(C_2H_4)_2]^{n+}$ with n=0 or 1, but accessible from a dicationic nickel (II) complex (Scheme 5, P,N=phosphino-iminophosphorane ligand).

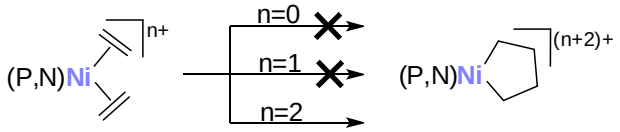

Scheme 5 – Theoretical studies on the accessibility of [nickellacycle]$^{(n+2)+}$ starting from a bis ethylene Ni^{n+} fragment. P,N=phosphino-iminophosphorane ligand.[32]

Several dicationic nickel complexes are already reported in literature.[33–37] However, they are stabilized by at least four strongly donating ligands, prohibiting ethylene coordination.

Inspired by these results, our goal was to synthesize a family of stable Ni complexes, able to generate the corresponding dicationic nickel fragment $[(L_2)Ni]^{2+}$,$2X^-$ upon activation. As this hypothetical species is expected to be highly Lewis acidic, careful choice of the counter ion was mandatory. The aluminate counter-anion $[Al(OR^F)_4]^-$ (R^F=$C(CF_3)_3$), reported to be one of the most weakly coordinating counter-anion in literature[38] and proton-free (avoid β-H at Ni),[39] appeared to be an excellent candidate for our purposes. We hypothesized that such $[Al(OR^F)_4]^-$ could be generated *in situ* via the abstraction of OR^{F-} from the $[(L_2)Ni(OR^F)_2]$ precursor using the highly Lewis acidic $(PhF)Al(OR^F)_3$ derivative reported by Krossing in 2008.[40] This strategy thus relied on a convenient access to a family of $[(L_2)Ni(OR^F)_2]$ complexes, two examples of which being known (L = PPh_3, Ph_3PO).[41]

We wish here to present first a new synthetic pathway to access $L_2Ni(OR^F)_2$ complexes from a "$Ni(OR^F)_2$" precursor. Secondly, we report the reactivity of $L_2Ni(OR^F)_2$/n $Al(OR^F)_3$ (n=1, 2, 4) systems under ethylene (Scheme 6), and demonstrate efficient oligomerization process, to form butenes and hexenes mixtures with selectivities in butenes in the 80-95% range. Isomerization of 1-butene to 2-butene was observed. This prompted an in-depth mechanistic study, which supports the formation of a "Ni-H" intermediate in the catalytic process.

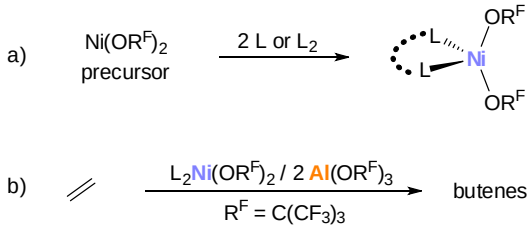

Scheme 6 – (a) Homoleptic monomeric alkoxy nickel complexes and their use in bis-alkoxy nickel synthesis in this work. (b) Dimerization of ethylene with $L_2Ni(OR^F)_2$/$Al(OR^F)_3$ systems. R^F=$C(CF_3)_3$.

RESULTS AND DISCUSSION

$[Ni(OR^F)_4]^{2-}$ synthesis

Several attempts to reach bis-alkoxy nickel complexes $[(L)Ni(OR^F)_2]$ have been made. The reaction between Cp_2Ni and an excess of perfluoro alcohol[42] and phosphine ligands (Ph_3P, Cy_3P) did not give expected results. Similarly, halogen substitution of chlorine from $NiCl_2$ complexes ($(dcpp)NiCl_2$, $(Cy_3P)_2NiCl_2$) with different MOR^F salts (M=Li, Na, Ag), only led to mixtures of complexes that could not be separated.

The reaction between $(DME)NiBr_2$ and $NaOR^F$ in DCM proved much more rewarding (Figure 1, top). Indeed, a deep blue solution was obtained after 4h at RT, while two different solids (white and yellow) precipitated from the solution, presumably NaCl and $NiBr_2$ respectively. The ^{19}F NMR of the crude mixture showed a major singlet at -35ppm, quite downfield shifted from free OR^{F-} (singlet around -70 to -75ppm)[43–46] attesting the coordination to a paramagnetic $Ni^{(II)}$ center. After workup to eliminate the solids, followed by evaporation, a deep blue solid was obtained. Deep blue crystals were obtained from a saturated pentane solution at 5°C. The X-ray structure analysis of **1** is shown in Figure 1 (bottom). It confirmed the formation of the homoleptic dianionic $[Ni(OR^F)_4]^{2-}$ nickel complex. Each OR^{F-} acts as bridging ligand between the Ni and Na centers. The anionic charges are compensated by two Na cations stabilized by DME molecules that can be observed in ^1H NMR as four broad signals at -5.8 (CH_3), -4.4 (CH_3), +6.0 (CH_2) and 10.5ppm (CH_2).

Ni-O bond length of complex **1** are 1.950(1) and 1.963(1)Å long, showing elongated sigma bonds (see ESI). The geometry of the $[Ni(OR^F)_4]^{2-}$ is identical to the one reported by Doerrer for $[Ni(OR^F)_4]K_2$ complex.[42] Complex **1** has a geometry at Ni between trigonal pyramidal and seesaw (O_1-Ni-O_2 = 116.45(4)°; τ_4=0.74).[47] The distorted geometry can be explained by the weak interaction with four fluorine atoms (Ni-F=2.932(1)Å and 3.009(1)Å), the bulkiness of the OR^F moieties and the presence of sodium cation in the structure. Each sodium cation appears to be hexacoordinated. It is being stabilized by four oxygen atoms (all Na-O bond range between 2.323(1) and 2.379(1)Å): two from OR^F moieties, and two from DME ligand, as well as two F atoms of the OR^F ligands. The Na-F distances (2.748(1) and

2.762(1)Å) are significantly longer than similar interaction reported by Miller (Na-F = 2.612(2)Å).[48]

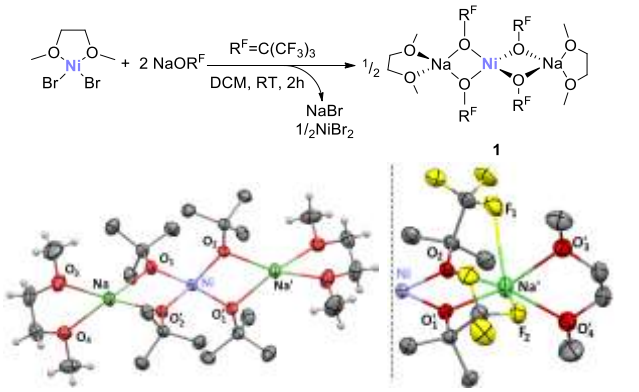

Figure 1 – Top : synthesis of complex **1**. Bottom: molecular structure of **1** in crystalline state. Thermal ellipsoids are drawn at 50% probability and F atoms are omitted for clarity. Distances [Å] and angles [°]: Ni-O_1 : 1.9498(8) ; Ni-O_2 : 1.9630(9) ; Na-O_1 : 2.3297(10) ; Na-O_3 : 2.3789(12) ; O_1-Ni-O_2 : 116.45(4) ; O_1-Ni-O_1' : 124.78(5) ; O_2-Ni-O_2' : 131.54(6).

In solution, this complex appears to be in equilibrium with other species, the amount of which depends on DME, THF (from the $NaOR^F$ reactant) and $NaOR^F$. Indeed, crystals dissolved in the DCM or *o*-DFB present minor signals (below 5% level) of one other OR^F moiety. This is however not an issue since after addition of ligands, only one compound is obtained (vide infra). Complex **1** is stable only in non-coordinating solvent (DCM, *o*-DFB, toluene, benzene, pentane). The use of coordinating solvents (such as THF or acetonitrile CH_3CN) did result in formation of mixtures of new complexes according to ^{19}F NMR spectroscopy (complete conversion in CH_3CN and partial conversion in THF). These results were highly positive as they clearly suggested that the OR^{F-} ligands in the $Ni(OR^F)_4^{2-}$ complex would be readily substituted by donating ligands.

Bis-alkoxy nickel complexes

Synthesis

We thus started the ligand substitution study by phosphine ligands. Two equivalents of Cy_3P were added to **1**. In DCM, the formation of $(Cy_3P)_2NiCl_2$ was evidenced by crystallization over one day, showing the unexpected full substitution of the OR^{F-} ligands, with chloride ligands obviously coming from the solvent. When *o*-DFB is used as a solvent, a purple solution was obtained instantaneously. No signals were observed in the ^{31}P NMR, attesting the coordination of Cy_3P to a paramagnetic Ni center. This was corroborated by ^{19}F NMR spectroscopy with the appearance of one singlet at -75ppm corresponding to the release of $(DME)NaOR^F$, and one singlet at -24 ppm, corresponding to the desired paramagnetic complex $(Cy_3P)_2Ni(OR^F)_2$ **2**.

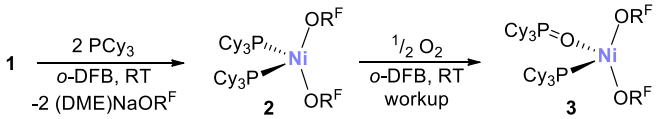

Scheme 7 – Synthesis of 2 by addition of 2 Cy_3P on 1 and its reactivity with traces of O_2 to reach 3. Workup = precipitation with pentane then filtration.

This complex proved however unstable. Indeed, a new signal at -17 ppm after workup appeared, and increased slowly at the expense of the signal at -24 ppm. The reaction was repeated and the formation of the new compound was followed by ^{19}F NMR (see ESI, figure S13). Over one week without workup, the complex featuring the signal at -17ppm had become the major compound. Single crystals were grown from a concentrated solution of *o*-DFB of this mixture. The X-ray structure analysis is disordered but clearly showed the presence of one oxidized phosphine Cy_3PO as well as a Cy_3P ligand both coordinated on Ni center (see ESI). The formula of the obtained crystalized complex can thus be written as $(Cy_3P)(Cy_3PO)Ni(OR^F)_2$ **3**. The experiment was repeated several times with increased efforts to prevent O_2 (thorough degassing) or H_2O contamination, yet identical results were observed. We believe this oxidation to be favored by the bulkiness of the Cy_3P phosphine[49] which prevents a strong coordination to the rather bulky $Ni(OR^F)_2$ moiety. The partial oxidation of the phosphine allows the strain relief and leads to a more stable complex (Scheme 7).

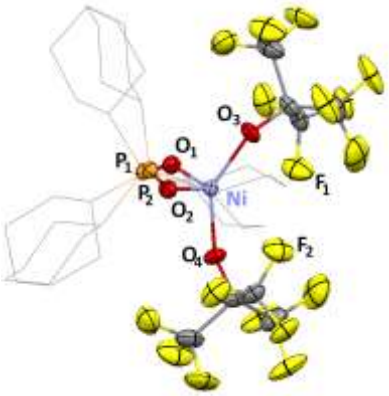

Figure 2 - Molecular structure of **4** in crystalline state. Thermal ellipsoids drawn at 50% probability, cyclohexyl groups simplified, H and disordered atoms omitted. Distances [Å] and angles [°] : Ni-O_1 = Ni-O_2 : 1.9570(7) ; Ni-O_3 : 1.9187(7) ; Ni-O_4 : 1.9188(7) ; P_1-O_1 : 1.5079(7) ; O_1-Ni-O_2 : 110.12(5) ; O_3-Ni-O_4 : 142.95 (5).

As phosphine oxides appeared to be good ligands for the "$Ni(OR^F)_2$" fragment, we studied the coordination of Cy_3PO. Two equivalents of Cy_3PO were added to a solution of complex **1** in *o*-DFB at RT, which gave a deep blue solution instantaneously. The release of $(DME)NaOR^F$ and formation of a new complex was observed by ^{19}F NMR as well as the formation of a new paramagnetic complex (δ = -11 ppm). No signal was observed in the ^{31}P NMR which confirmed the coordination of Cy_3PO on Ni. Single crystals were grown from a saturated solution of pentane/*o*-DFB at -35°C, and $(Cy_3PO)_2Ni(OR^F)_2$ complex **4** was isolated in 92% yield. Its 3D structure is presented on Figure 2.

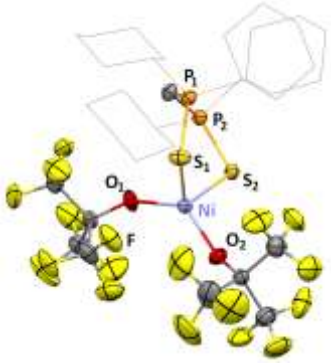

Figure 3 - Molecular structure of **5** in crystalline state. Thermal ellipsoids drawn at 50% probability cyclohexyl groups simplified, H and disordered atoms omitted. Distances [Å] and angles [°] : Ni-O_1 : 1.8828(12) ; Ni-O_2 : 1.9199(13) ; Ni-S_1 : 2.3202(5) ; Ni-S_2 : 2.3275(5) ; P_1-S_1 : 1.9864(6) ; O_1-Ni-O_2 : 130.54(6) ; S_1-Ni-S_2 : 105.36(2).

Coordination of weaker ligands featuring P=S bonds was studied. If the coordination of monodentate Cy_3PS on **1** did not occur, as shown by ^{31}P NMR, the one of the bidentate ligand bis-(dicyclohexylphosphino)-methane disulfide (dcpmS) readily occurred. Indeed, when adding this bidentate PS ligand to complex

1, a change of color to deeper blue was noticed instantaneously. The lack of ^{31}P NMR signal pointed again the formation of a paramagnetic complex **5**. XRD analysis on single crystals grown from a saturated pentane/o-DFB at -35°C solution (Figure 3) proved the synthesis of the desired (dcpmS)Ni(OR^F)$_2$ complex (88% yield).

In order to further evaluate the effect of steric bulk on the coordination of phosphine ligands, other bidentate ligands were used. 5 min. after the addition of bis(dicyclohexylphosphino) propane (dcpp) on **1** in *o*-DFB at RT, a purple solution was obtained. In addition, a novel singlet at -22 ppm attributed to (dcpp)Ni(OR^F)$_2$ (**6**) was observed in the ^{19}F NMR spectrum, along with the signal of free (DME)NaOR^F. This complex proved rather sensitive to hydrolysis. Indeed, crystallization of the crude mixture from a saturated solution of pentane/*o*-DFB at -35°C resulted in the formation of (dcpp)Ni(OR^F)(OH).R^FOH **7** as orange crystals within 16h at -35°C (Scheme 8, left). Interestingly, letting the same solution 16 more hours at RT allowed the solubilization of previously formed orange crystals followed by the crystallization of insoluble dimeric compound **8** [(dcpp)Ni(μ-O)]$_2$, (Scheme 8 , right). A square planar geometry around the nickel is observed for both complexes **7** and **8** (τ_4=0). Crystals of complex **9**.R^FOH were solubilized in C_6D_6 and ^{19}F NMR showed that there was an equilibrium between **6** (-22ppm) and **7**.R^FOH (-76 (br) & -75 (s) ppm). The formation of the insoluble complex **10** results from the full hydrolysis of two Ni-OR^F moieties. This unusual reactivity (Scheme 8, top) was unexpected in light of the differences in the pKa of R^FOH (5.6 in H_2O, 10.7 in DMSO) and H_2O (14.0 in H_2O, 32 in DMSO).[50] This reactivity is proposed to result from the stronger donation from hydroxo and oxo ligands compared to OR^{F-}. The presence of the other strong field ligand dcpp, results in the favored square planar geometry at Ni.

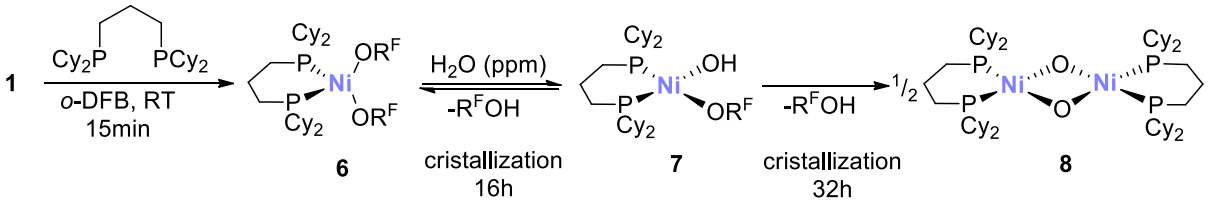

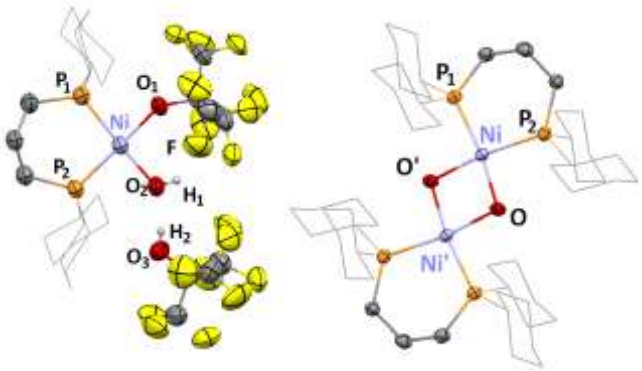

Scheme 8 – Top: Formation of dimer 8 from successive reaction of supposed (dcpp)Ni(OR^F)$_2$ with traces of water. Down: Molecular structure of 7 and 8 in crystalline state. Thermal ellipsoids drawn at 50% probability, cyclohexyl groups simplified. H, disordered atoms and solvent molecule (8) omitted. (except H on O in 7). Distances [Å] and angles [°] : compound 7 (left) : Ni-O_1 : 1.926(2) ; Ni-O_2 : 1.895(3) ; Ni-P_1 : 2.182(1) Ni-P_2 : 2.174(1) ; O_1-Ni-O_2 : 94.72(10) ; P_1-Ni-P_2 : 96.82(4) ; O_1-Ni-P_1 : 82.27(8) ; O_2-Ni-P_2 : 86.18(8). Compound 8 (right) : Ni-O : 1.902(4) ; Ni-O' : 1.909(4) ; Ni-P_1 : 1.175(2) ; Ni-P_2 : 2.174(2) ; P_1-Ni-O : 170.60(12) ; P_2-Ni-O' : 171.36(12).

The hydrolysis of the Ni-OR^F bond appeared to depend also on the steric bulk of the strong field ligand diphosphine. Indeed, in the case of bis-(diphenylphosphino) ferrocene (dppf), no such side reaction occurred. Thus, the addition of one equiv. of dppf on **1** in *o*-DFB gave a dark orange solution. A new signal at -25 ppm was observed beside the signal of (DME)NaOR^F, attesting the formation of the complex (dppf)Ni(OR^F)$_2$ **9** which did not evolve in days (isolated in 83% yield). Single crystals suitable for X-ray diffraction analysis were grown from a pentane solution at room temperature. The structure is shown on Figure 4.

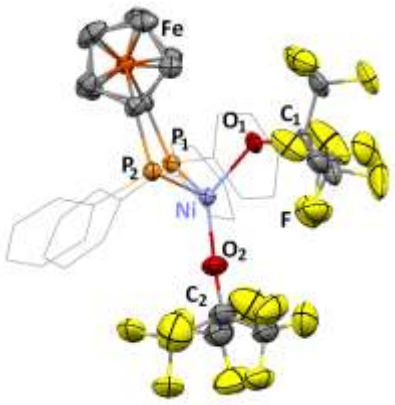

Figure 4 - Molecular structure of **9** in crystalline state. Thermal ellipsoids drawn at 50% probability, phenyl groups simplified. H, disordered atoms and solvent molecule omitted. Distances [Å] and angles [°] : Ni-O_1 : 1.937(2) ; Ni-O_2 : 1.868(2) ; Ni-P_1 : 2.356(1) ; Ni-P_2 : 2.358(1) ; O_1-Ni-O_2 : 132.1(2) ; P_1-Ni-P_2 : 102.8(1) ; Ni-O_1-C_1 : 133.5(2) ; Ni-O_2-C_2 : 165.2(3).

Finally, to extend the family of bis-alkoxy nickel complexes, the coordination of N ligands, i.e. bipyridine ligands was studied. The coordination of bipyridine or 4,4'-substituted bipyridine gave intractable mixtures. On the other hand, coordination of 2,2'-dimethyl-6,6'-bipyridine ($bipyMe_2$) proved to be selective. Indeed, the addition of one equivalent of $bipyMe_2$ on **1** in *o*-DFB at RT gave an orange solution. As observed for **2**, **3** and **4**, two singlets were obtained in the ^{19}F NMR spectrum. The signal of $(bipyMe_2)Ni(OR^F)_2$ **10** was located at -49 ppm and the release of $(DME)NaOR^F$ was again evidenced by a singlet at -75ppm. Single crystals were grown from a saturated solution of pentane/*o*-DFB. The structure of **10**, isolated in 98% yield, is presented on Figure 5.

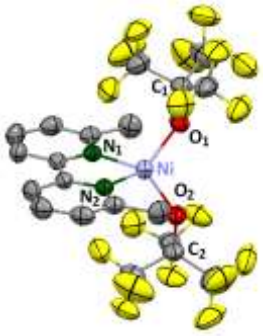

Figure 5 - Molecular structure of **10** in crystalline state. Thermal ellipsoids drawn at 50% probability, H and disordered atoms omitted. Distances [Å] and angles [°] : Ni-O_1 = Ni-O_2 : 1.8933(17) ; Ni-N_1 = Ni-N_2 : 1.990(2) ; P_1-S_1 : 1.9864(6) ; O_1-Ni-O_2 : 109.73(11) ; N_1-Ni-N_2 : 82.76 (11).

X-Ray Diffraction analyses

Not surprisingly, the geometries at Ni in these complexes depend on the ligands. No square planar geometries are observed for the monomeric complexes, likely due to the bulkiness of the OR^F groups. In the case of **5** and **10**, where dcpmS and $bipyMe_2$ are the ligands, the geometry around nickel is trigonal pyramidal with τ_4=0.87 for **5** and τ_4=0.85 for **8**. For **4** (Cy_3PO) and **9** (dppf), a geometry between seesaw and trigonal pyramidal is noticed (τ_4=0.76 for **4** and 0.73 for **9**). Nickel oxygen bonds lengths vary between 1.868(2)Å and 1.937(2)Å, for complex **9**. These values are longer than most reported Ni-O bond length (median value for Ni-O bond length: 1.85Å, see ESI, figure S15), due to the presence of electron-withdrawing and bulky $C(CF_3)_3$ moieties. In complexes **5** and **9**, the two Ni-O bond distances are different. Notably, in complex **9** the two Ni-O bond distances are different by 0.07Å. In this case, the shortest Ni-O_2 bond is linked to a wider Ni-O_2-C_2 angle of 165.2(3)° *vs* 133.5(2)° for Ni-O_1-C_1, pointing a stronger Ni-O interaction.

Ni-F interactions are observed in the solid-state structure (Ni-F_1 = NiF_2: 2.840(3)Å (**4**); 2.825(3)Å (**7**); 2.973(2)Å (**9**)). Considering these interactions, the geometry around these complexes are pseudo-octahedral for **4** and **5** and pseudo-square pyramidal for **9** (τ_5=0.33).[51] Except for complex **5** (dcpmS) that have long Ni-S bonds (2.320(1) and 2.328(1)Å) compared to literature (*ca* 2.20Å, only four structures with square planar geometry at Ni),[52] all L-Ni bonds have standard lengths compared to previously reported $Ni^{(II)}$ complexes featuring these ligands.[53–55] PO and PS bonds are slightly elongated in complexes **4** and **5** compared to the free ligand (+0.02 to 0.03Å),[56] due to the coordination on nickel.

Stability

While complex **10** was stable in all tested solvents, complexes **4**, **5** and **9** were not stable in coordinating solvents. In fact, their dissolution in ACN or THF immediately released the corresponding ligand (detected by ^{31}P NMR) and several new Ni complexes were observed in the ^{19}F NMR spectra (signals not attributed).

In accord with the observed instability of $[(dcpp)Ni(OR^F)_2]$ toward water, all complexes degraded under air or upon contact with water.

The four isolated $L_2Ni(OR^F)_2$ complexes obtained from the unique precursor $[Ni(OR^F)_4][Na(DME)]_2$ **1** are exposed on Scheme 9 as a general scheme for this synthetic part.

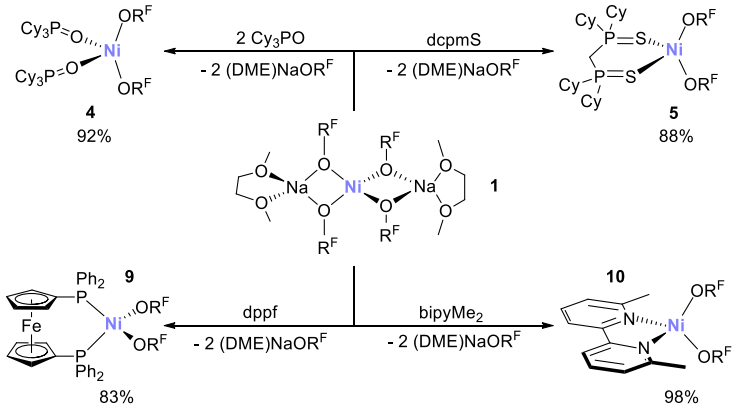

Scheme 9 – Overview of all isolated bis-alkoxy nickel complexes.

Reactivity toward ethylene

All complexes were tested in ethylene oligomerization after activation with different equivalents of $PhF{\rightarrow}Al(OR^F)_3$ (PhF=fluorobenzene) in *o*-DFB (*Table 1*). This strong Lewis acid, reported by Krossing,[40] was freshly prepared before each catalytic test by addition of 3.1 eq. of R^FOH (in *o*-DFB) on $AlEt_3$ (in fluorobenzene) at -40°C. The obtained colorless solution was immediately introduced in the reactor at 25°C to avoid known decomposition of the Lewis acid.[57] Indeed, the introduction of the Lewis acid on a solution at 50°C led to absence of activity most likely due to fast decomposition of the Lewis acid, before reacting with $L_2Ni(OR^F)_2$ (entry 1). Therefore, the quantity of catalyst and solvent used, as well as the overall pressure were adapted depending on the activity of the produced systems, to avoid exotherms. The blank reactions, where the nickel precursors and $PhF{\rightarrow}Al(OR^F)_3$ were tested alone under ethylene (5 bar in pressure NMR tubes), did not present any activity.

We first focused on finding the best catalytic conditions with complex **10** as the precursor (entries 1-4). The addition of only one equivalent of $PhF{\rightarrow}Al(OR^F)_3$ was not sufficient to induce significant activity (entry 2), suggesting the cationic $[L_nNiOR^F]^+$ fragment not to be an active species. On the other hand, the use of two equivalents of Lewis acid led to much higher activity (entry 3). It has to be noted that the consumption over time was

constant (see ESI, figure S21), proving the formation of a very robust system. Disappointingly, the hypothetical formation of the envisioned dicationic $[L_nNi]^{2+}$ fragment under these conditions did not lead to high selectivity for 1-butene, that would be expected if a metallacyclic pathway was followed. Increasing the number of equivalents of Al from 2 to 4 did not have any effect on the selectivity but decreased the activity in dimerization (entry 4). Therefore, in the subsequent tests, activation of $L_2Ni(OR^F)_2$ precursor was carried out with only two equivalents of $Al(OR^F)_3$.

The ligand influence was notable as activities differed very significantly depending on the precursor. Similar isomerization pattern was observed with the different starting precatalysts which can be attributed to similar active species. Complex **10** ($bipyMe_2$ ligand) was found to be the least active precursor. Indeed, complex **5** (dcpmS ligand) was more than twice as active as **10** (entry 5 *vs.* 3). Complexes **4** (Cy_3PO) and **9** (dppf) were too active at the optimal conditions determined for **10** (20 bar, 25°C, 20mL of solvent) and the temperature could not be controlled (exotherm of 45°C and 58°C respectively). When decreasing the pressure (10 bar), the exotherm was lower for **4** (18°C, entry 6), leading to a much higher activity compared to complex **10** (entries 6 *vs* 9; 23918 *vs* 1159 $g_{C2H4}.g_{Ni}.h^{-1}$) although a higher isomerization was measured (34% 1-butene vs 52%). The exotherm under these conditions with complex **9** was of 44°C, being too high for gathering exploitable data. Finally, increasing the volume of solvent (20 to 30 mL) prevented such exotherms and provided activity and selectivity values that can be compared (entry 7, 8 and 10). Under these conditions, catalysis with complex **9** (dppf) led to the best activity of our complexes (entry 8, 50774 $g_{C2H4}.mol_{Ni}.h^{-1}$). These results clearly showed the influence of the ligand in the activity, being in the order: dppf>>Cy_3PO>dcpmS>$bipyMe_2$. In all tested conditions, selectivity for butenes range from moderate to excellent (73-97%). Unfortunately, the selectivity in 1-butene is quite low (not higher than 53% in the butene fraction for activity higher than 5000 $g_{C2H4}.g_{Ni}.h^{-1}$).

Catalytic tests with $(dppf)NiCl_2$ and $(bipyMe_2)NiCl_2$ (entry 14 and 15 respectively), activated by ethyl aluminium dichloride (EADC) were carried out to compare activity and selectivity with $L_2Ni(OR^F)_2/2Al(OR^F)_3$ catalytic systems. For dppf ligand (entry 8 *vs* 14), selectivity in butenes were similar (*ca* 80%) while isomerization was higher starting from the $(dppf)Ni(OR^F)_2$ precursor (27.7 vs 51.2% 1-butene). In the case of $bipyMe_2$ (entry 3 *vs* 15), selectivity in butenes is *ca* 20% lower with $(bipyMe_2)NiCl_2$/EADC (75.2%) than with $(bipyMe_2)Ni(OR^F)_2/Al(OR^F)_3$ (91.3%) while selectivity in 1-butene is better for the former (60.7 *vs* 51.9%).

Table 1 – Catalytic tests with $L_2Ni(OR^F)_2/Al(OR^F)_3$, L_2 : $(Cy_3PO)_2$, $bipyMe_2$, dppf, dcpmS; $(dppf)NiCl_2$/EADC and $(bipyMe_2)NiCl_2$/EADC.

Entry	Precursor (µmol)	$Al(OR^F)_3$ (µmol)	Additive (µmol)	Activity ($kg_{C2H4}.g_{Ni}.h^{-1}$)	%butenes (%b1)	%hexenes (%h1)
1	**12** (50)[a]	100	-	0	-	-
2	**12** (50)	50	-	traces	98.2 (75.0)	-
3	**12** (50)	100	-	10.7	91.3 (51.9)	7.0 (13.2)
4	**12** (50)	200	-	4.6	89.4 (52.8)	7.6 (16.3)
5	**7** (50)	100	-	26.9	77.8 (43.2)	15.5 (7.6)
6	**6** (10)[b]	20	-	23.9	73.2 (34.4)	19.1 (6.5)
7	**6** (10)[b,c]	20	-	7.7	91.0 (60.8)	7.7 (14.0)
8	**11** (10) [b,c]	20	-	50.8	80.3 (27.7)	13.2 (7.2)
9	**12** (50)[b]	100	-	1.2	97.2 (52.4)	1.8 (16.7)
10	**12** (50)[b,c]	100	-	1.1	93.6 (66.5)	5.1 (16.7)
11	**12** (50)	100	R^FOH (50)	9.1	89.9 (50.7)	8.2 (12.8)
12	**12** (50)[d]	100	H_2O (40)	0	-	-
13	**12** (50)[d,e]	100	H_2O (10)	1.1	82.9 (52.7)	13.5 (13.5)
14	$(dppf)NiCl_2$ (2.5)[e]	-	EADC (37.5)	87.8	84.7 (51.2)	14.4 (14.4)
15	$(bipyMe_2)NiCl_2$ (2.5)[e]	-	EADC (37.5)	21.1	75.2 (60.7)	23.7 (16.3)

General conditions: addition at 25°C of freshly prepared PhF→$Al(OR^F)_3$ in PhF/*o*-DFB on a solution of $L_2Ni(OR^F)_2$ saturated in C_2H_4. *o*-DFB (total of solution: 20mL), 25°C, 20 bar. Catalysis are stopped after 15-17g of consumed ethylene or after 1h by quenching with amines. [a]Addition of $Al(OR^F)_3$ at 50°C. [b]Catalytic tests done at 10 bar. [c]Volume of solvent = 30mL. [d]Wet *o*-DFB is added on the precursor, under ethylene and before activation with $Al(OR^F)_3$.[e]No activity after 15min at 25°C. Ethylene consumption started when heating at 50°C. [e]Cyclohexane is used as solvent and catalysis done at 50°C (not active at 25°C).

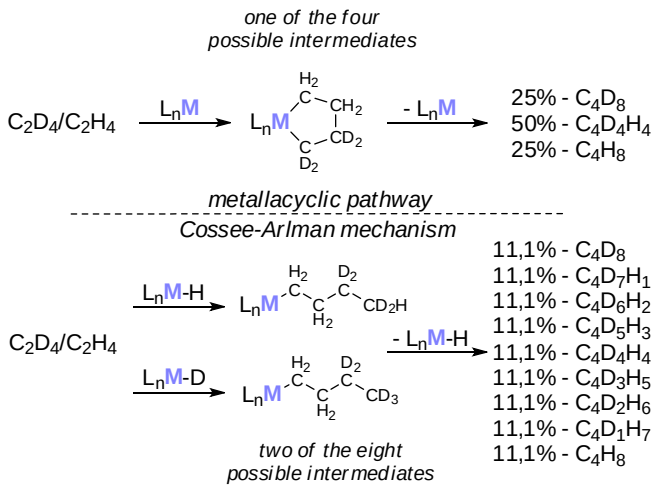

Scheme 10 – 1-butene isotopomers depending on followed mechanisms: Cossee-Arlman vs. metallacycle. These isotopomers mixtures lead to drastically different mass spectrum (cf. Figure 6).[58]

The good activity and selectivity in butenes formation of some complexes contrasted with the poor selectivity in the desired 1-butene. We therefore became interested in the mechanism followed by these complexes. Oligomerization tests with a mixture of C_2H_4 and C_2D_4 with a 1:1 ratio, as described by Bercaw[59] and McGuinness,[58,60] were carried out. Indeed, these authors have shown that the theoretical mass spectra of 1-butene depended on the mechanism of the catalytic process, Cossee-Alrman vs. metallacyclic. For the latter, only three different isotopomers are produced (C_4H_8, $C_4H_4D_4$, C_4D_8) while all possible 1-butene isotopomers are produced during a Cossee-Arlman mechanism (Scheme 10).[58] It has to be noted that theoretical mass spectrum of butenes from Cossee-Arlman mechanism did not take into account a "hydrogen scrambling" process (vide infra). These different isotopomers mixtures obviously led to different mass spectrum which were theoretically determined (Figure 6, grey and pale orange). Thus, catalytic tests were done in NMR tubes in o-DFB/PhF (9/1), under pressures from 2 to 2.5 bar, with different ratios of complex **10** (1µmol) to PhF→Al(OR^F)$_3$ (1:2, 1:4). The ethylene consumption was followed by ^{2}H NMR and when enough butenes were produced, typically within 5min, a GC-MS analysis of the gas phase was done. In all cases the mass spectrum of butenes fraction was identical and presented on Figure 6 (blue). The first important information was that beyond 2:1, the ratio of Lewis acid to precatalyst had no impact on the final mass distribution of butenes.

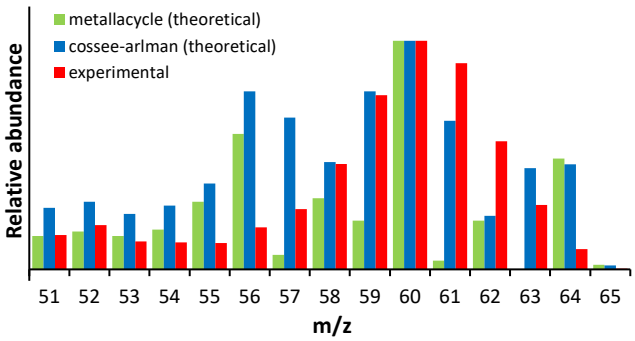

Figure 6 – Mass spectrum of 1-butene after catalysis under C_2H_4/C_2D_4 (1/1, 2.5b) with **10**/2Al(OR^F)$_3$ system in o-DFB at RT.

Strikingly also, our experimental spectra did not match either of the two theoretical distributions of Cossee-Arlman and metallacyclic mechanisms. Nevertheless, this behavior was previously described by Britovsek for catalysts that oligomerize ethylene through a Cossee-Arlman mechanism.[61] They showed that a fast H/D scrambling could occur on ethylene once a cationic M-H fragment was formed, that resulted in coexistence of M-D, M-H complexes and mixtures of partially labelled ethylene substrates $C_2D_{4-x}H_x$ (see ESI, figure S28). This observation was consistent with fast successive insertion/β-H elimination processes at the Ni-ethyl stage (Scheme 11). The similarity of our results with the ones of Britovsek clearly suggests the formation of a [Ni-H] complex from the (bipyMe$_2$)Ni(OR^F)$_2$ precatalyst upon reaction with two equivalents of PhF→Al(OR^F)$_3$, thereby ruling out the metallacyclic mechanism.

Such a formation of a [Ni-H] species was puzzling and prompted further experiments. The first hypothesis was that the H from Ni-H bond came from C_2H_4. The same experiment was therefore carried out under deuterated ethylene (purity: 99.99%). The mass spectrum of the 1-butene fraction showed, among the various m/z, the presence of small yet significant amounts of several odd mass compounds, the most abundant being C_4D_7H (4.2%, Figure 7). Although being in minor amount, the presence of that product demonstrates the formation of a Ni-H intermediate under pure C_2D_4, and not only the expected Ni-D that would result from C-D activation.

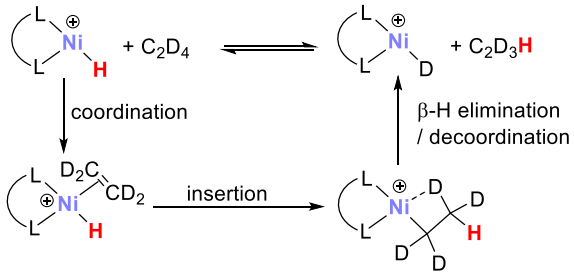

Scheme 11 – H/D scrambling at the Ni-ethyl stage.

Therefore, upon activation, a small quantity of a "Ni-H" complex did not come from ethylene. A second plausible hypothesis was that minute amounts of acidic species were responsible for Ni-H formation. A slight excess of alcohol (3.1 eq. of R^FOH are used to generate PhF→Al(OR^F)$_3$) was first supposed to be the source of proton. If it were the case, more R^FOH should increase the amount of Ni-H and thereby the activity in ethylene oligomerization. However, when doing the catalytic test with one more equivalent of alcohol (entry 11 *vs.* 3), a slight *decrease* in activity was observed while keeping similar selectivity behavior. Similarly, the catalysis in the presence of different amounts of water were carried out, leading to lack of activity with either 0.2 and 0.8 eq. of H_2O (*vs* catalyst, entries 13 and 12 resp.) in the solvent. These results did not conclude whether or not the "acids" were the source of hydride. Indeed, a competition between inhibition by coordination of the Lewis base (R^FOH and H_2O) and formation of Ni-H can explain the lack of activity in both cases. In summary, these mechanistic investigations have evidenced the intermediacy of a [Ni-H] moiety in a Cossee-Arlman mechanism. Deuterium labelling rules out the involvement of ethylene in the formation of such [Ni-H] intermediate.

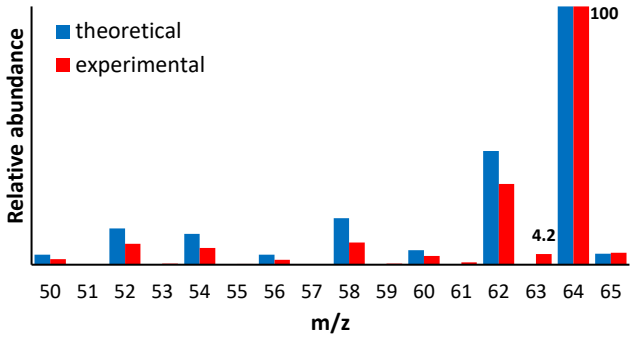

Figure 7 - Mass spectrum of 1-butene after catalysis under C_2D_4 (2.5b) with **10**/2Al(OR^F)$_3$ system in o-DFB at RT.

CONCLUSION

In conclusion, we have reported the synthesis of the novel tetra-alkoxy nickelate complex [Ni(OR^F)$_4$][Na(DME)]$_2$. We demonstrated the latter to be a convenient precursor for the L_2Ni(OR^F)$_2$ family after selective double OR^F- substitutions with electronically and sterically different L ligands (monodentate and bidentate ligands). We therefore believe this reaction to be very general, providing access to a wide family of L_2Ni(OR^F)$_2$ complexes from this precursor. We then tested four L_2Ni(OR^F)$_2$ complexes in ethylene oligomerization, after activation with the Al(OR^F)$_3$ Lewis acid, leading to good to excellent activity and selectivity in butenes. The selectivity in 1-butene was nevertheless disappointingly low, in apparent disagreement with the foreseen metallacyclic mechanism. Mechanistic studies, involving the use of C_2H_4/C_2D_4 and C_2D_4 coupled with GC-MS analysis evidenced the formation of minor amounts of a [Ni-H] intermediate, whose source is still unclear and under investigation in our groups. It is likely that this complex is responsible for the isomerization of 1-butene into 2-butene. Work is currently being carried out in our laboratories focusing on the generation of the active species "L_2Ni^{2+}" from the L_2Ni(OR^F)$_2$ precursors, *without* generating the "Ni-H" intermediate, to probe the accessibility and efficiency of the metallacyclic mechanism in the oligomerization process.

ASSOCIATED CONTENT

Supporting Information

The Supporting Information is available free of charge on the ACS Publications website.

Full experimental details, additional experiments, NMR spectra and XRD details (PDF)

AUTHOR INFORMATION

Corresponding Author

* Nicolas Mézailles
mezailles@chimie.ups-tlse.fr

*Lionel Magna
Lionel.magna@ifpen.fr

Notes

The authors declare no conflict of interest.

ACKNOWLEDGMENT

For financial support of this work, we acknowledge IFP Energies Nouvelles. We thank David Proriol and Emmanuel Pellier for their technical support for the H/D scrambling studies and oligomerization experiments.

REFERENCES

(1) Young, C. T.; von Goetze, R.; Tomov, A. K.; Zaccaria, F.; Britovsek, G. J. P. The Mathematics of Ethylene Oligomerisation and Polymerisation. *Top. Catal.* **2020**, *63*, 294–318. https://doi.org/10.1007/s11244-019-01210-0.

(2) Arlman, J.; Cossee, P. Ziegler-Natta Catalysis III. Stereospecific Polymerization of Propene the Catalyst System TiCl3-AlEt3. *J. Catal.* **1964**, *3*, 99–104.

(3) Bre, A.; Chauvin, Y.; Commereuc, D. Mode of Decomposition of Titanacyclopentanes, Model of the Intermediates Species in the Dimerization of Olefins Catalyzed by Titanium Complexes. *New J. Chem.* **1986**, *10*, 535–537.

(4) Mcguinness, D. S. Olefin Oligomerization via Metallacycles: Dimerization, Trimerization, Tetramerization, and Beyond. *Chem. Rev.* **2011**, *111*, 2321–2341. https://doi.org/10.1021/cr100217q.

(5) Sydora, O. L. Selective Ethylene Oligomerization. *Organometallics* **2019**, *38* (5), 997–1010. https://doi.org/10.1021/acs.organomet.8b00799.

(6) Breuil, P.-A. R.; Magna, L.; Olivier-Bourbigou, H. Role of Homogeneous Catalysis in Oligomerization of Olefins : Focus on Selected Examples Based on Group 4 to Group 10 Transition Metal Complexes. *Catal. Letters* **2015**, *145* (1), 173–192. https://doi.org/10.1007/s10562-014-1451-x.

(7) Keim, W.; Kowaldt, F. H.; Goddard, R.; Krüger, C. Novel Coordination of (Benzoylmethylene)Triphenylphosphorane in a Nickel Oligomerization Catalyst. *Angew. Chemie Int. Ed.* **1978**, *17* (6), 466–467. https://doi.org/10.1002/anie.197804661.

(8) Keim, W. Oligomerization of Ethylene to α-Olefins: Discovery and Development of the Shell Higher Olefin Process (SHOP). *Angew. Chemie - Int. Ed.* **2013**, *52*, 12492–12496. https://doi.org/10.1002/anie.201305308.

(9) Olivier-Bourbigou, H.; Breuil, P. A. R.; Magna, L.; Michel, T.; Espada Pastor, M. F.; Delcroix, D. Nickel Catalyzed Olefin Oligomerization and Dimerization. *Chem. Rev.* **2020**, *120*, 7919–7983. https://doi.org/10.1021/acs.chemrev.0c00076.

(10) Miiller, U.; Keim, W.; Krüger, C.; Betz, P. [(Ph2PCH2C(CF3)2O)NiH(PCy3)] : Support for a Nickel Hydride Mechanism in Ethene Oligomerization. *Angew. Chemie - Int. Ed.* **1989**, *28*, 1011–1013.

(11) Lhermet, R.; Moser, E.; Jeanneau, E.; Breuil, P.; Olivier-bourbigou, H. Complexes Outer-Sphere Reactivity Shift of Secondary Phosphine Oxide-Based Nickel Complexes : From Ethylene Hydrophosphinylation to Oligomerization. *Chem. - A Eur. J.* **2017**, *23*, 7433–7437. https://doi.org/10.1002/chem.201701414.

(12) Buchard, A.; Auffrant, A.; Klemps, C.; Vu-do, L.; Le Goff, X. F.; Le Floch, P. Highly Efficient P – N Nickel (II) Complexes for the Dimerisation of Ethylene. *Chem. Commun.* **2007**, *15*, 1502–1504. https://doi.org/10.1039/b618401d.

(13) Mukherjee, S.; Patel, B. A.; Bhaduri, S. Selective Ethylene Oligomerization with Nickel Oxime Complexes. *Organometallics* **2009**, *28* (10), 3074–3078. https://doi.org/10.1021/om900080h.

(14) Zhang, J.; Liu, S.; Li, A.; Ye, H.; Li, Z. Nickel(II) Complexes Chelated by 2,6-Pyridinedicarboxamide: Syntheses, Characterization, and Ethylene Oligomerization. *New J. Chem.* **2016**, *40*, 7027–7033. https://doi.org/10.1039/c6nj00559d.

(15) Boulens, P.; Pellier, E.; Jeanneau, E.; Reek, J. N. H.; Hélène, O.-B.; Breuil, P.-A. R. Self-Assembled Organometallic Nickel Complexes as Catalysts for Selective Dimerization of Ethylene into 1-Butene. *Organometallics* **2015**, *34*, 1139–1142. https://doi.org/10.1021/acs.organomet.5b00055.

(16) Feng, C.; Zhou, S.; Wang, D.; Zhao, Y.; Liu, S.; Li, Z.; Braunstein, P. Cooperativity in Highly Active Ethylene Dimerization by Dinuclear Nickel Complexes Bearing a Bifunctional PN Ligand. *Organometallics* **2021**, *40* (2), 184–193.

https://doi.org/10.1021/acs.organomet.0c00683.

(17) Antonov, A. A.; Semikolenova, N. V.; Soshnikov, I. E.; Talsi, E. P.; Bryliakov, K. P. Selective Ethylene Dimerization into 2-Butenes Using Homogeneous and Supported Nickel(II) 2-Iminopyridine Catalysts. *Top. Catal.* **2020**, *63* (1–2), 222–228. https://doi.org/10.1007/s11244-019-01208-8.

(18) Otten, E.; Batinas, A. A.; Meetsma, A.; Hessen, B. Versatile Coordination of Cyclopentadienyl-Arene Ligands and Its Role in Titanium-Catalyzed Ethylene Trimerization. *J. Am. Chem. Soc.* **2009**, *131* (14), 5298–5312. https://doi.org/10.1021/ja810089f.

(19) Agapie, T.; Labinger, J. A.; Bercaw, J. E. Mechanistic Studies of Olefin and Alkyne Trimerization with Chromium Catalysts: Deuterium Labeling and Studies of Regiochemistry Using a Model Chromacyclopentane Complex. *J. Am. Chem. Soc.* **2007**, *129* (46), 14281–14295. https://doi.org/10.1021/ja073493h.

(20) Hoyt, J. M.; Schmidt, V. A.; Tondreau, A. M.; Chirik, P. J. Iron-Catalyzed Intermolecular [2+2] Cycloadditions of Unactivated Alkenes. *Science*, **2015**, *349*, 960–963. https://doi.org/10.1126/science.aac7440.

(21) Sattler, A.; Labinger, J. A.; Bercaw, J. E. Highly Selective Olefin Trimerization Catalysis by a Borane-Activated Titanium Trimethyl Complex. *Organometallics* **2013**, *32* (23), 6899–6902. https://doi.org/10.1021/om401098m.

(22) Arteaga-Müller, R.; Tsurugi, H.; Saito, T.; Yanagawa, M.; Oda, S.; Mashima, K. New Tantalum Ligand-Free Catalyst System for Highly Selective Trimerization of Ethylene Affording 1-Hexene: New Evidence of a Metallacycle Mechanism. *J. Am. Chem. Soc.* **2009**, *131* (15), 5370–5371. https://doi.org/10.1021/ja8100837.

(23) Chen, Y.; Callens, E.; Abou-Hamad, E.; Merle, N.; White, A. J. P.; Taoufik, M.; Copéret, C.; Le Roux, E.; Basset, J. M. [(≠SiO)TaVCl2Me2]: A Well-Defined Silica-Supported Tantalum(V) Surface Complex as Catalyst Precursor for the Selective Cocatalyst-Free Trimerization of Ethylene. *Angew. Chemie - Int. Ed.* **2012**, *51* (47), 11886–11889. https://doi.org/10.1002/anie.201206272.

(24) Sattler, A.; Aluthge, D. C.; Winkler, J. R.; Labinger, J. A.; Bercaw, J. E. Enhanced Productivity of a Supported Olefin Trimerization Catalyst. *ACS Catal.* **2016**, *6* (1), 19–22. https://doi.org/10.1021/acscatal.5b02604.

(25) Steelman, D. K.; Aluthge, D. C.; Lehman, M. C.; Labinger, J. A.; Bercaw, J. E. Mechanistic Studies on Selective Trimerization of Linear α-Olefins over a Supported Titanium Catalyst. *ACS Catal.* **2017**, *7* (8), 4922–4926. https://doi.org/10.1021/acscatal.7b00256.

(26) Ohashi, M.; Shirataki, H.; Kikushima, K.; Ogoshi, S. Nickel-Catalyzed Formation of Fluorine-Containing Ketones via the Selective Cross-Trimerization Reaction of Tetrafluoroethylene, Ethylene, and Aldehydes. *J. Am. Chem. Soc.* **2015**, *137*, 6496–6499. https://doi.org/10.1021/jacs.5b03587.

(27) Binger, P.; Doyle, M. J.; McMeeking, J.; Krüger, C.; Tsay, Y.-H. Metallacycloalkanes I. Preparation and Characteriation of a,a'-Bipyridyl-5-Nickela-3,3,7,7-Tetramethyl-Trans-Tricyclo[4.1.0.0]Heptane. *J. Organomet. Chem.* **1977**, *135*, 405–414. https://doi.org/10.1016/S0022-328X(00)88092-4.

(28) Doyle, M. J.; McMeeking, J.; Binger, P. Nickelacyclopentane Derivatives as Intermediates in the Nickel(0)-Catalysed Cyclodimerisation of Strained-Ring Olefins. *J. Chem. Soc. Chem. Commun.* **1976**, No. 11, 376–377. https://doi.org/10.1039/C39760000376.

(29) Grubbs, R. H.; Miyashita, A.; Liu, M.-I. M.; Burk, Patrick, L. The Preparation and Reactions of Nickelocyclopentanes. *J. Am. Chem. Soc.* **1977**, *99*, 3863–3864.

(30) Binger, P.; Doyle, M. J. Metallacycloalkanes. II. Reactions of α,A'-Bipyridyl-5-Nickela-3,3,7,7-Tetramethyl-Trans-Tricyclo[4.1.0.02,4]Heptane. *J. Organomet. Chem.* **1978**, *162* (2), 195–207. https://doi.org/10.1016/S0022-328X(00)82038-0.

(31) Ohashi, M.; Kawashima, T.; Taniguchi, T.; Kikushima, K.; Ogoshi, S. 2,2,3,3-Tetrafluoronickelacyclopentanes Generated via the Oxidative Cyclization of Tetrafluoroethylene and Simple Alkenes: A Key Intermediate in Nickel-Catalyzed C−C Bond-Forming Reactions. *Organometallics* **2015**, *34*, 1604–1607. https://doi.org/10.1021/acs.organomet.5b00218.

(32) Tognetti, V.; Buchard, A.; Auffrant, A.; Ciofini, I.; Le Floch, P.; Adamo, C. Ethylene Dimerization Catalyzed by Mixed Phosphine – Iminophosphorane Nickel (II) Complexes : A DFT Investigation. *J. Mol. Model.* **2013**, *19*, 2107–2118. https://doi.org/10.1007/s00894-012-1631-9.

(33) Schwab, M. M.; Himmel, D.; Kacprzak, S.; Radtke, V.; Kratzert, D.; Yassine, Z.; Weis, P.; Weber, S.; Krossing, I. Reactivity of [Ni(COD)2][Al(ORF)4] towards Small Molecules and Elements. *Zeitschrift fur Anorg. und Allg. Chemie* **2018**, *644* (1), 50–57. https://doi.org/10.1002/zaac.201700367.

(34) Yang, J. Y.; Bullock, R. M.; Shaw, W. J.; Twamley, B.; Fraze, K.; DuBois, M. R.; DuBois, D. L. Mechanistic Insights into Catalytic H2 Oxidation by Ni Complexes Containing a Diphosphine Ligand with a Positioned Amine Base. *J. Am. Chem. Soc.* **2009**, *131* (16), 5935–5945. https://doi.org/10.1021/ja900483x.

(35) Ganushevich, Y.; Miluykov, V.; Yakhvarov, D.; Sinyashin, O.; Lönnecke, P.; Hey-Hawkins, E. Novel Halogen-Bridged Bisphosphine Nickel(II) Complexes. *Inorganica Chim. Acta* **2011**, *376* (1), 118–122. https://doi.org/10.1016/j.ica.2011.06.007.

(36) Weiss, C. J.; Das, P.; Miller, D. L.; Helm, M. L.; Appel, A. M. Catalytic Oxidation of Alcohol via Nickel Phosphine Complexes with Pendant Amines. *ACS Catal.* **2014**, *4* (9), 2951–2958. https://doi.org/10.1021/cs500853f.

(37) Wang, X.; Liu, S.; Jin, G. X. Preparation, Structure, and Olefin Polymerization Behavior of Functionalized Nickel(II) N-Heterocyclic Carbene Complexes. *Organometallics* **2004**, *23* (25), 6002–6007. https://doi.org/10.1021/om049467.

(38) Riddlestone, I. M.; Kraft, A.; Schaefer, J.; Krossing, I. Taming the Cationic Beast: Novel Developments in the Synthesis and Application of Weakly Coordinating Anions. *Angew. Chemie - Int. Ed.* **2018**, *57* (43), 13982–14024. https://doi.org/10.1002/anie.201710782.

(39) Cornella, J.; Gómez-Bengoa, E.; Martin, R. Combined Experimental and Theoretical Study on the Reductive Cleavage of Inert C-O Bonds with Silanes: Ruling out a Classical Ni(0)/Ni(II) Catalytic Couple and Evidence for Ni(I) Intermediates. *J. Am. Chem. Soc.* **2013**, *135*, 1997–2009. https://doi.org/10.1021/ja311940s.

(40) Müller, L. O.; Himmel, D.; Stauffer, J.; Steinfeld, G.; Slattery, J.; Santiso-Quiñones, G.; Brecht, V.; Krossing, I. Simple Access to the Non-Oxidizing Lewis Superacid PhF→Al(OR F)3 (RF = C (CF3)3). *Angew. Chemie - Int. Ed.* **2008**, *47* (40), 7659–7663. https://doi.org/10.1002/anie.200800783.

(41) Brazeau, S. E. N.; Pope, F.; Huang, V. L.; Anklin, C.; Rheingold, A. L.; Doerrer, L. H. Phosphine Ligands as Protecting Groups for 3d Complexes in Oxidation by O2. *Polyhedron* **2020**, *186*, 114609. https://doi.org/10.1016/j.poly.2020.114609.

(42) Zheng, B. N.; Miranda, M. O.; DiPasquale, A. G.; Golen, J. A.; Rheingold, A. L.; Doerrer, L. H. Synthesis and Electronic Spectra of Fluorinated Aryloxide and Alkoxide [NiX4]2- Anions. *Inorg. Chem.* **2009**, *48* (10), 4274–4276. https://doi.org/10.1021/ic9003593.

(43) Krossing, I. The Facile Preparation of Weakly Coordinating Anions: Structure and Characterisation of Silverpolyfluoroalkoxyaluminates AgAl(ORF)4, Calculation of the Alkoxide Ion Affinity. *Chem. - A Eur. J.* **2001**, *7* (2), 490–502. https://doi.org/10.1002/1521-3765(20010119)7:2<490::AID-CHEM490>3.0.CO;2-I.

(44) Boudjelel, M.; Zhai, F.; Schrock, R. R.; Hoveyda, A. H.; Tsay, C. Oxo 2-Adamantylidene Complexes of Mo(VI) and W(VI). *Organometallics* **2021**, *40*, 838–842. https://doi.org/10.1021/acs.organomet.1c00086.

(45) Lum, J. S.; Tahsini, L.; Golen, J. A.; Moore, C.; Rheingold, A. L.; Doerrer, L. H. K...F/O Interactions Bridge Copper(I) Fluorinated Alkoxide Complexes and Facilitate Dioxygen Activation. *Chem. - A Eur. J.* **2013**, *19*, 6374–6384. https://doi.org/10.1002/chem.201204275.

(46) Qiao, L.; Cui, Z.; Chen, B.; Xu, G.; Zhang, Z.; Ma, J.; Du, H.; Liu, X.; Huang, S.; Tang, K.; Dong, S.; Zhou, X.; Cui, G. A Promising Bulky Anion Based Lithium Borate Salt for Lithium Metal Batteries. *Chem. Sci.* **2018**, *9* (14), 3451–3458. https://doi.org/10.1039/c8sc00041g.

(47) Yang, L.; Powell, D. R.; Houser, R. P. Structural Variation in Copper(I) Complexes with Pyridylmethylamide Ligands: Structural Analysis with a New Four-Coordinate Geometry Index, T4. *J. Chem. Soc. Dalt. Trans.* **2007**, No. 9, 955–964.

https://doi.org/10.1039/b617136b.

(48) Smith, J. B.; Kerr, S. H.; White, P. S.; Miller, A. J. M. Thermodynamic Studies of Cation-Macrocycle Interactions in Nickel Pincer-Crown Ether Complexes Enable Switchable Ligation. *Organometallics* **2017**, *36*, 3094–3103. https://doi.org/10.1021/acs.organomet.7b00431.

(49) Tolman, C. A. Phosphorus Ligand Exchange Equilibria on Zerovalent Nickel. A Dominant Role for Steric Effects. *J. Am. Chem. Soc.* **1970**, *92*, 2956–2965. https://doi.org/10.1021/ja00713a007.

(50) Bordwell, F. G. Equilibrium Acidities in Dimethyl Sulfoxide Solution. *Acc. Chem. Res.* **1988**, *21* (12), 456–463. https://doi.org/10.1021/ar00156a004.

(51) Addison, A. W.; Rao, T. N. Synthesis, Structure, and Spectroscopic Properties of Copper(II) Compounds Containing Nitrogen-Sulfur Donor Ligands ; the Crystal and Molecular Structure of Aqua[1,7-Bis(N-Methylbenzimidazol-2'-Yl)-2,6-Dithiaheptane]Copper(II) Perchlorate. *J. Chem. Soc. Dalt. Trans.* **1984**, No. 1, 1349–1356.

(52) Hu, P.; Yao, Z. J.; Wang, J. Q.; Jin, G. X. Synthesis, Structure, and Olefin Polymerization Behavior of Nickel Complexes with Carborane [S,C] or [S,S] Ligands. *Organometallics* **2011**, *30*, 4935–4940. https://doi.org/10.1021/om200516b.

(53) Casellato, U.; Ajó, D.; Valle, G.; Corain, B.; Longato, B.; Graziani, R. Heteropolymetallic Complexes of 1,1′-Bis(Diphenylphosphino) Ferrocene (Dppf). II. Crystal Structure of Dppf and NiCl2(Dppf). *J. Crystallogr. Spectrosc. Res.* **1988**, *18* (5), 583–590. https://doi.org/10.1007/BF01161151.

(54) Serrano, E.; Martin, R. Nickel-Catalyzed Reductive Amidation of Unactivated Alkyl Bromides. *Angew. Chemie - Int. Ed.* **2016**, *55*, 11207–11211. https://doi.org/10.1002/anie.201605162.

(55) Poulten, R. C.; Lo, I.; Llobet, A.; Mahon, M. F.; Whittlesey, M. K. Stereoelectronic Effects in C−H Bond Oxidation Reactions of Ni(I) N-Heterocyclic Carbene Complexes. *Inorg. Chem.* **2014**, *53*, 7160–7169.

(56) Davies, J. A.; Dutremez, S.; Pinkertin, A. A. Solid-State 31P NMR and X-Ray Crystallographic Studies of Tertiary Phosphines and Their Derivatives. *Inorg. Chem.* **1991**, *30*, 2380–2387.

(57) Kraft, A.; Trapp, N.; Himmel, D.; Böhrer, H.; Schlüter, P.; Scherer, H.; Krossing, I. Synthesis, Characterization, and Application of Two Al(ORF)3 Lewis Superacids. *Chem. - A Eur. J.* **2012**, *18* (30), 9371–9380. https://doi.org/10.1002/chem.201200448.

(58) Suttil, J. A.; McGuinness, D. S. Mechanism of Ethylene Dimerization Catalyzed by Ti(OR′)4/AlR3. *Organometallics* **2012**, *31* (19), 7004–7010. https://doi.org/10.1021/om3008508.

(59) Agapie, T.; Schofer, S. J.; Labinger, J. A.; Bercaw, J. E. Mechanistic Studies of the Ethylene Trimerization Reaction with Chromium-Diphosphine Catalysts: Experimental Evidence for a Mechanism Involving Metallacyclic Intermediates. *J. Am. Chem. Soc.* **2004**, *126* (5), 1304–1305. https://doi.org/10.1021/ja038968t.

(60) Overett, M. J.; Blan, K.; Bollmann, A.; Dixon, J. T.; Haasbroek, D.; Killian, E.; Maumela, H.; McGuinness, D. S.; Morgan, D. H. Mechanistic Investigations of the Ethylene Tetramerisation Reaction. *J. Am. Chem. Soc.* **2005**, *127* (30), 10723–10730. https://doi.org/10.1021/ja052327b.

(61) Tomov, A. K.; Gibson, V. C.; Britovsek, G. J. P.; Long, R. J.; Van Meurs, M.; Jones, D. J.; Tellmann, K. P.; Chirinos, J. J. Distinguishing Chain Growth Mechanisms in Metal-Catalyzed Olefin Oligomerization and Polymerization Systems: C2H4/C 2D4 Co-Oligomerization/Polymerization Experiments Using Chromium, Iron, and Cobalt Catalysts. *Organometallics* **2009**, *28* (24), 7033–7040. https://doi.org/10.1021/om900792x.